

# We are IntechOpen, the world's leading publisher of Open Access books Built by scientists, for scientists

6,900

Open access books available

186,000

International authors and editors

200M

Downloads

Our authors are among the

154

Countries delivered to

TOP 1%

most cited scientists

12.2%

Contributors from top 500 universities



WEB OF SCIENCE™

Selection of our books indexed in the Book Citation Index  
in Web of Science™ Core Collection (BKCI)

Interested in publishing with us?  
Contact [book.department@intechopen.com](mailto:book.department@intechopen.com)

Numbers displayed above are based on latest data collected.  
For more information visit [www.intechopen.com](http://www.intechopen.com)



# Design Principles of 5G NR RoF-Based Fiber-Wireless Access Network

*Mikhail E. Belkin, Tatiana N. Bakhvalova  
and Alexander S. Sigov*

## Abstract

For today, much attention in the upcoming 5G New Radio (NR) mobile networks is paid to radically expanding the available spectral bands up to millimeter wavelengths (MMW). Following this tendency, currently, the local telecommunication commissions of various countries are proposing and harmonizing the plans of frequency allocation in MMW band, which will be reviewed this year at the World Radio Conference (WRC-2019). Another milestone of great importance is the development of access networks. Here, well-known radio-over-fiber (RoF) technology is considered as the most promising approach, which is implemented based on fiber-wireless (FiWi) architecture. Elaborating the direction, in this chapter we review the worldwide progress of RoF-architected 5G NR access networks and highlight our last simulation results on design and optimization of millimeter-phonic-based FiWi interface. All schemes are modeled using VPIphotonics Design Suite software tool. In the result of simulation experiments, optimal design principles of optical distribution network (ODN), fiber-wireless interface (FWI), and fiber-wireless fronthaul network (FWFN) as a whole have been proposed, described, and validated.

**Keywords:** 5G NR mobile communication system, access network, RoF technology, millimeter-wave fiber-wireless architecture, computer-aided design

## 1. Introduction

Within the recent decades, an explosion of researches and developments referring to the next-generation communication networks known as 5G New Radio (NR) has been observed [1–5]. Based on 4G long-term evolution (LTE) progress [6], 5G NR is in principle a novel stage of unprecedented technological innovation with ubiquitous speed connectivity. As a result, it is expected that 5G NR will radically transform a number of industries and will provide direct, superspeed connections between any users, sensors, and devices.

At the present time, several reviews to analyze significant changes in the 5G NR approaches as compared to the existing 4G LTE networks have been published [7, 8] denoting a series of milestones. Among them, much attention is paid to radically expanding the available spectral bands up to millimeter wavelengths (MMW). Following this tendency, currently, the local telecommunication

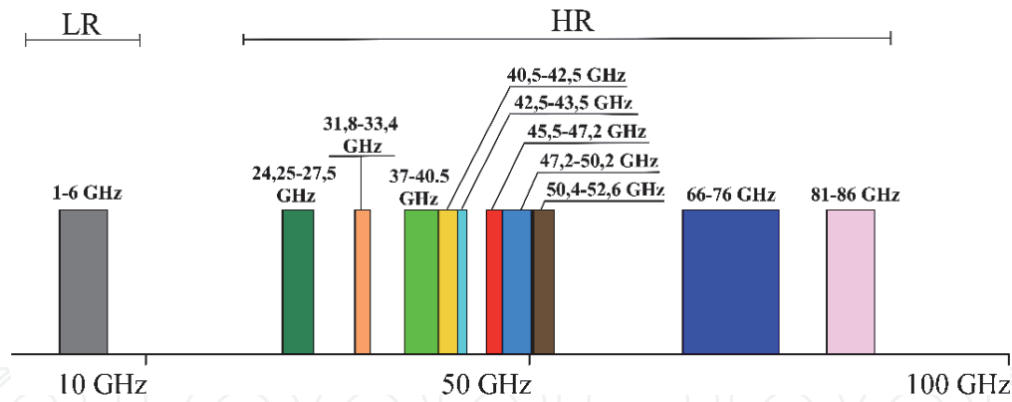


**Figure 1.**  
Planned 5G NR spectrum allocations [10].

commissions of various countries are proposing and harmonizing the plans of frequency allocation in microwave band that has to be coexistent with 4G LTE and in newer MMW band, which will be reviewed this year at the World Radio Conference (WRC-2019) [9]. However, **Figure 1** shows a preliminary frequency plan [10] sharing two separate sub-bands: the so-called low range (LR) inside 1–6 GHz and the high range (HR) inside 24–86 GHz.

Another milestone of great importance is the development of access networks. In this direction, the well-known radio-over-fiber (RoF) technology [11–13] is considered as the most promising approach, which is implemented based on fiber-wireless (FiWi) architecture.

Following them, recently we contributed some works referred to design microwave-photonic-based MMW FiWi interface [14–24]. Elaborating the direction, in this chapter we review the worldwide progress of RoF-architected 5G NR access networks and highlight our last simulation results on design and optimization of photonic-based FiWi interface. In this way, the rest of the chapter is organized as follows. Section 2 reviews the distinctive features of access networks for 5G NR mobile communication systems including small cell scenario, RoF concept, and microwave-photonic-based approach to construct the network equipment. A specific example illustrating a RoF-based small cell scenario in 5G NR network is also included. In addition, Section 3 presents the results of our recent investigations to design optimally a fiber-wireless fronthaul network (FWFN) including an optical distribution network (ODN) and MMW fiber-wireless interface (FWI). All schemes are modeled using off-the-shelf VPIphotonics Design Suite software tool. Finally, Section 4 concludes the chapter.

## 2. The distinctive features of access networks for 5G NR mobile communication systems

Generally, low transmission loss and broad bandwidth characteristics of optical fibers, possibility of wavelength division multiplexing, and low sensitivity to electromagnetic interference of optical fiber-based transmission systems allow the introduction of novel concepts into distribution and processing of the digital signals being transmitted over a communication network. One of the most important examples of introducing radically new approaches is the upcoming mobile network 5G NR. According to the Introduction, a number of new principles are introduced in 5G NR network design. Three of the most suitable for access networks will be discussed below.

2.1 Small cell scenario

In the last decade, the problem of developing and optimizing the architecture of the fifth-generation communication networks and developing equipment for their implementation has received the closest attention of the global telecom community [6]. It is predicted that the implementation of these next-generation networks will provide unprecedented amounts of data and services for mobile and fixed users, which can be called both an evolution and a revolution in mobile cell technologies [1]. They are architectural in nature—for example, moving some decision-making to the devices themselves (device-centric architectures and smart devices)—or most networks are hardware-oriented. Besides, continuously increasing requirements for broadband services and capacity of communication links by enhancing the data transfer rate in all sections of the cellular network led to the shift of the operating frequency to millimeter-wave band, with a total cell capacity of several gigabits per second. One of the keys of them is ultra-densification of service areas and users. The data obtained from the analysis of a large number of publications, on the quantitative parametric comparison for mobile communication networks of the available fourth and incoming fifth generations, are presented in **Table 1**.

To ensure so sharp explosion of the key parameters, a significant complication of the standard cellular network structure is required. Thus, according to the generally accepted opinion, the ambitious goals for the development of fifth-generation wireless networks can be achieved by solving two advanced global tasks: architectural one, associated with the small cell scenario for access network, and the technological one, associated with the introduction of microwave-photonic (MWP) approach to the design of the network equipment. The further is connected with the introduction of the fronthauls based on FiWi architecture. The latter is especially important for interface network units, both between the fiber-optic backhaul network and fronthaul networks, whose task is to transfer high-speed data stream to millimeter-wave carriers, and between wired and wireless sections of the access network, in which the signals of the optical and millimeter-wave bands should be cost-efficiently converted. As an example of implementing small cell scenario concept, an advanced skeleton diagram of 5G NR network using a common central station (CS), fiber backhauls, and FiWi fronthauls is shown in **Figure 2**.

2.2 Radio-over-fiber concept

Analyzing the parameters of **Table 1**, one can make the following clear conclusion. More than an order of magnitude increased requirements to throughput make fiber-optic communication system as a leading technology not only for transport networks but also for next-generation access networks. However, the important

Parameter	4G LTE	5G NR
Connection density (per km <sup>2</sup> )	Less 200 K	Up to 1 M
End-to-end latency (ms)	>50	<1
User mobility (km/h)	Up to 80	Up to 500
Peak data rate in cell (Gbit/s)	<1	>20
Traffic volume density (Tbit/s/km <sup>2</sup> )	<1	Up to 10 s
User experienced data rate (Gbit/s)	<0.1	Up to 1

**Table 1.**  
*A comparison of the key parameters achieved in the 4G LTE mobile networks with similar parameters to be achieved in the 5G NR networks.*

drawback for the implementation of the latter ones is the complexity and high cost associated with the need to lay the optical cables up to user terminals. In contrast, current wireless access networks that provide a flexible connection with a relatively simple infrastructure cannot meet growing in geometric progression demands to increase the capacity of mobile communication systems. The most promising technique to meet it, which is actively discussed in the referred publications, is to implement radio-over-fiber (RoF) network concept with FiWi architecture and to expend the operating frequency band up to millimeter waves (MMW) applying multi-position digital modulation on a radio-frequency (RF) carrier [25, 26].

**Figure 3** shows a typical configuration of a RoF-based communication network including central station (CS) and set of remote (base) stations (RS), which are a key element of a RoF-based fiber-wireless fronthaul network (FWFN) that

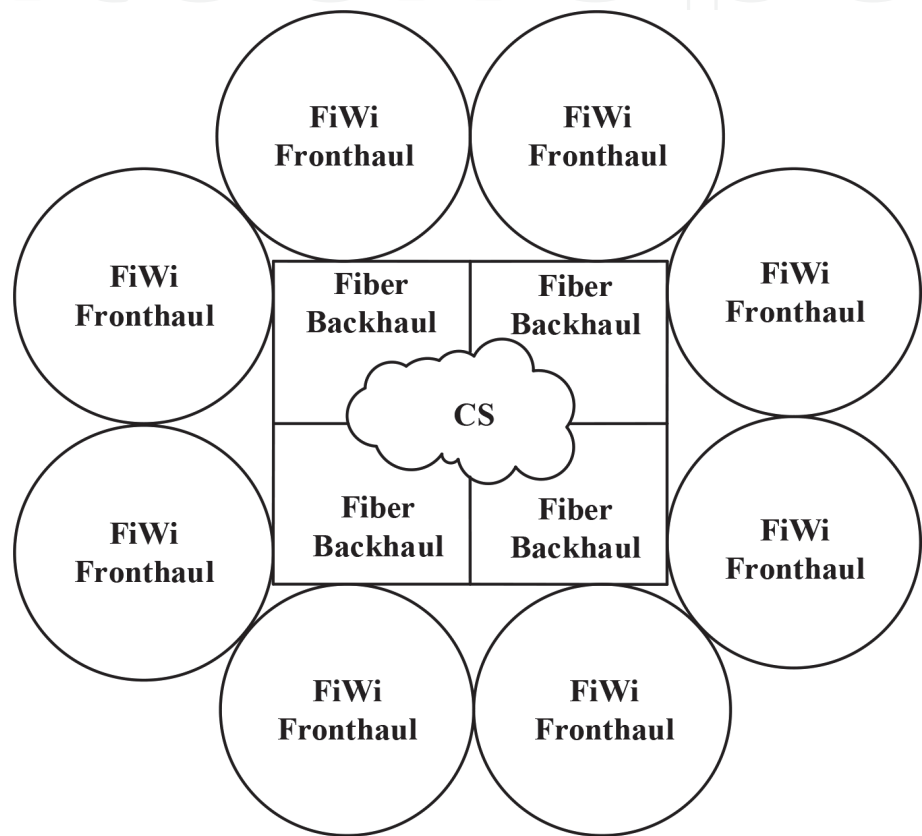


**Figure 2.**  
*Skeleton diagram for 5G NR cellular communication network.*

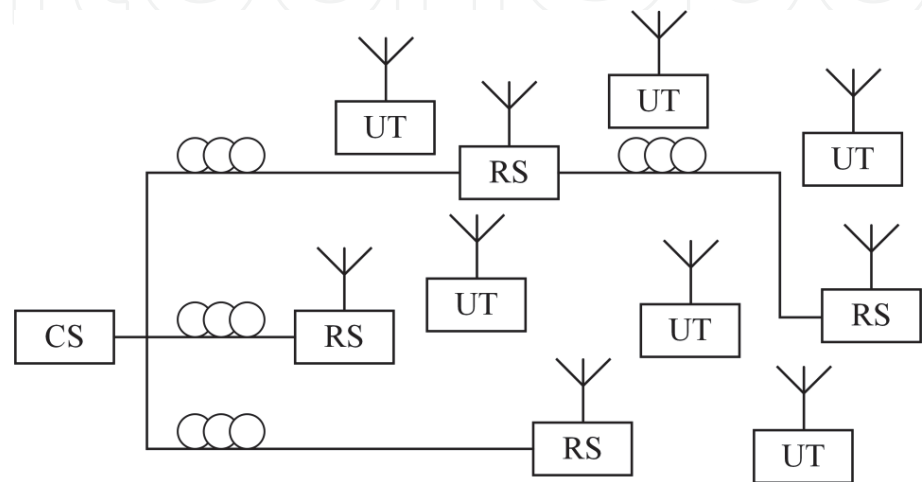


**Figure 3.**  
*A conceptual diagram of a RoF-based mobile communication network.*



interactively (using downlink and uplink) connects the CS and each RS using fiber fronthaul links (FFL) and microwave or millimeter-wave band user radio terminals (UT). As is known, for the transmission of signals through a FFL, direct and inverse electro-optical conversions are required. The first one in the RoF-based communication system is usually performed with the help of an external electro-optical modulator (EOM) and the second with a photodetector.

In the framework of RoF concept, combining MMW band and FiWi network architecture inside FWFN is one of the promising ways to deliver intensive digital traffic with seamless convergence between wired optical backhaul and fiber-wireless fronthaul. In addition, FiWi technique allows converting directly a lightwave spectrum to MMW radio spectrum using a simple microwave-photonic-based up-/down-conversion scheme, which is important to keep the remote cells flexible, cost-effective, and power-efficient. **Figure 4** exemplifies a MMW-band FiWi architecture, in which CS is interactively connected with pico-cell's RSs through fiber-optic link. A typical position of RS is in the center of the service area; that is, for omnidirectional covering, four phased array antennas (PAAs) with an azimuth of  $90^\circ$  would be an optimal decision [16].

2.3 Example of a 5G NR network using small cell scenario and RoF concept

Let us illustrate small cell scenario using an example of building a backhaul network in a specific medium-scale city. **Figure 5** depicts 5G's backhaul fiber-optic network consisting of one macro-cell with service diameter of 5.3 km, inside of

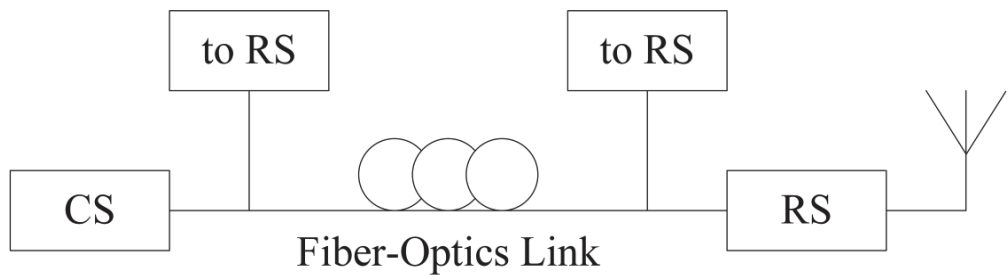


**Figure 4.**  
*A conceptual diagram of a RoF-based MMW fiber-wireless fronthaul network.*

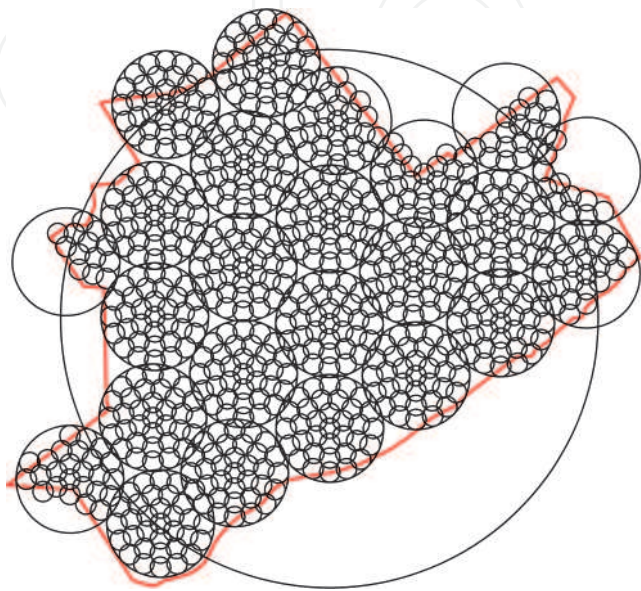


**Figure 5.**  
*5G's backhaul fiber-optic network of a medium-scale city.*

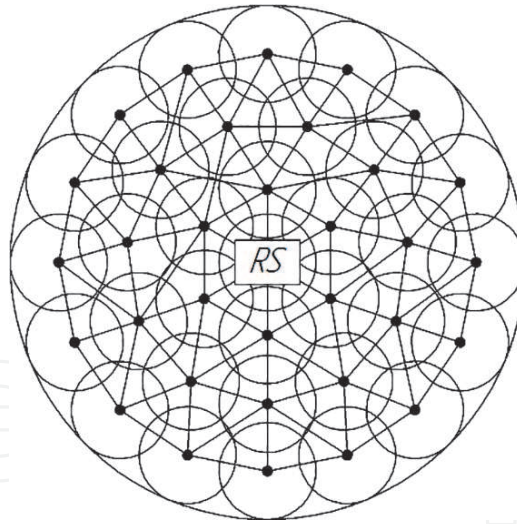


**Figure 6.**  
*Conceptual diagram of pico-cells inside one micro-cell.*

which 24 micro-cells of service diameter near 1 km are located. The red line marks the boundaries of the city.

Introducing a smaller partition, **Figure 6** shows a typical micro-cell diagram containing 33 pico-cells with a 200-m service diameter. In the center of each pico-cell, a remote station (RS) is located (see **Figure 3**), which is an interface between fiber and wireless network sections. A bold dot indicates it. All RSs are interactively interconnected via fiber-optic lines, forming a communication structure of the type “fully connected network.”

## 2.4 Microwave-photonic-based approach

### 2.4.1 The area of microwave photonics

Microwave photonics (MWP) is a multidisciplinary research and industrial field encompassing optical, microwave and radio frequency (RF), and electrical researchers and engineers ([5, 20, 21, 26] and refs. cited there). This field in the last 30 years has attracted immense interest and generated many new R&Ds from both the scientific community and the commercial sector. Emerging applications for mobile communication network of FiWi architecture, sub-terahertz wireless systems, radar, and electronic warfare systems indicate that MWP is a subject of importance. By common opinion, MWP opens the way to superwide bandwidth characteristics at lower size, weight, and power as compared with traditional means [11]. For example, **Figure 7** depicts typical arrangements of MWP-based software-defined RF receiving (a) and transmitting (b) units. As it follows, a photonic circuit is inserted between two microwave electronic chains. For direct and inverse transformations of microwave and optical signals, there are two interfacing units at their bounds: electrical-to-optical (E/O) and optical-to-electrical (O/E) converters. Between the interfaces, there are various photonic processing units for switching, distribution, filtration, time delaying, and up/down frequency conversion of microwave signals in optical domain.

### 2.4.2 Millimeter-wave photonic technique in fiber-wireless-interfaced 5G wireless networks

To implement effective radio communication within small cell scenario, a number of leading countries developed a prospective spectrum including MMW bands up to 100 GHz (see **Figure 1**). As shown in numerous studies, MMW 5G network

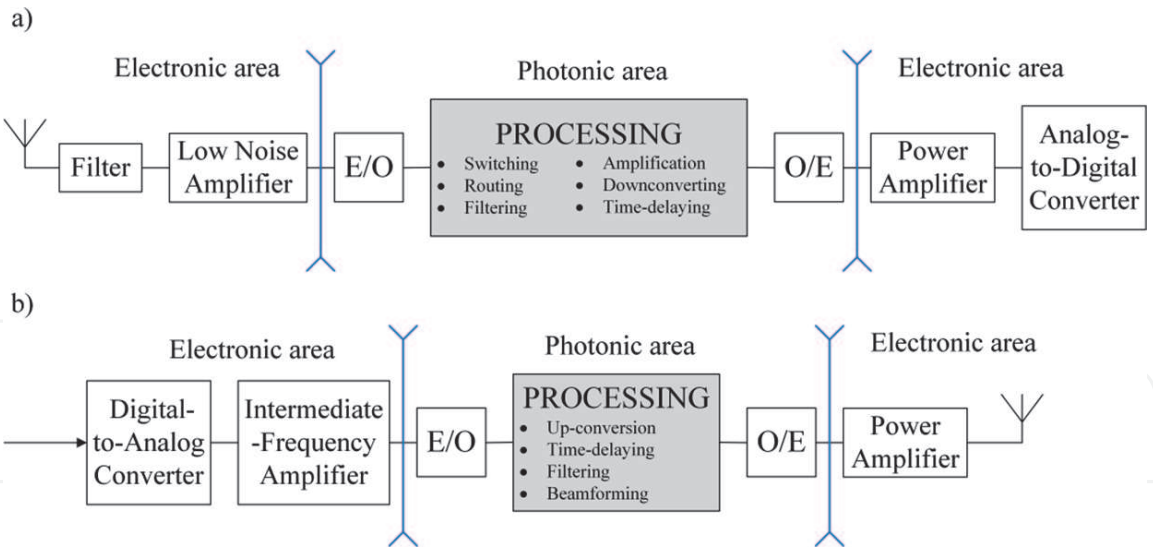


**Figure 7.**  
*A typical arrangement of MWP-based RF receiver (a) and transmitter (b).*

infrastructure must be shared with a lot of small service zones controlled by the corresponding RS. In order to avoid inter-interference in these zones, one of the feasible approaches is to provide the RS with beam-steerable PAAs [16].

Generally, to form directional beams for transmission and receiving signals from adjacent UTs and RSs, MMW RS must use PAA with hundreds of antenna elements. In addition, FiWi technique allows converting directly a lightwave spectrum to MMW radio spectrum using a simple MWP-based up-conversion scheme [16], which is important to keep the remote cells flexible, cost-effective, and power-efficient and support seamless FWFN.

### 3. Design principles of fiber-wireless fronthaul network

In general, the fronthaul network of FiWi architecture represents the further development of cellular communication networks. The peculiarity of construction in comparison with the traditional system of cellular communication is in a much smaller area of cells down to pico-cells for mobile UTs with service diameter not more than 200 m and to femto-cells for indoor distribution with service diameter from tens of centimeters to 20–50 m. Due to the relatively small number of UTs inside the cell, it is critical to reduce cost of RS equipment, in fact, representing an effective interface between the optical and RF sections of the transmission system. The most promising solution to this problem is the ultimate simplification of the RS layout, which could be done by shifting all the processing procedures to the CS. If someone analyzes the diagram of **Figure 4** addressed to FWFN, from the functional viewpoint, two sub-systems are liberated that consist of optical distribution network (ODN) including CS hardware and fiber-optic link (FOL) and fiber-wireless interface (FWI) including a RS hardware and the same FOL. The proposed design principle is clearly illustrated in **Figure 8**.

The key advantages of the FiWi architecture for the communication networks are the following [1–4, 7]:

- Higher noise immunity, since data streams are mainly delivered through FOLs
- Small attenuation of signal power in fiber-based transmission path due to the fact that the losses in the fiber-optic cable are four orders of magnitude smaller than in the coaxial one



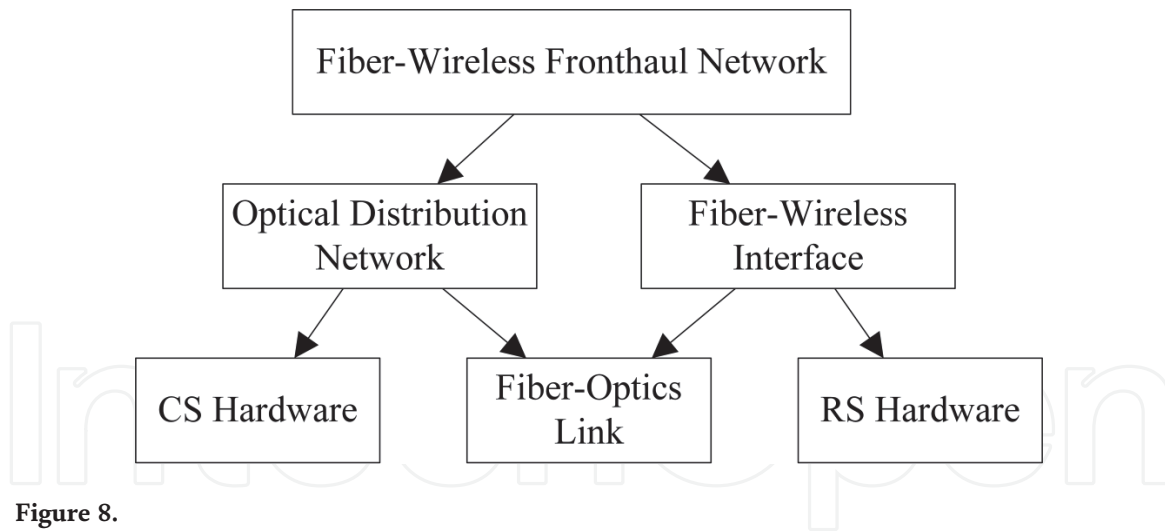


**Figure 8.**  
The design principle of fiber-wireless fronthaul network.

- Relative simplicity of implementation and deployment at site by applying a remote base station concept that can service a significant number of wireless UTs
- A lower cost of construction and operation that simplifies the structure and reduces the power consumption of RSs due to using in the access networks the principle of transmission of digital streams on the carriers of the RF band
- Great future-proof design due to the fact that the ultra-wideband fiber-optic communication links guarantee minimal additional capital investments to upgrade the network throughput

Based on the benefits noted above, the next subsections review the principles, features, and ways to advance design of fifth-generation RoF-based access network using FiWi architecture.

### 3.1 Design of optical distribution network

As follows from the above discussion, the key function of the CS is the efficient electro-optical conversion. In this way, below we check by the simulation a CS for a RoF-based mobile network so to determine a feasible modulation method and the device for its realization when using optical transmission of multi-position quadrature amplitude modulation (QAM) of RF signals over FFL under investigation. Specifically, below we examine comparatively two key methods of optical modulation:

- Direct intensity modulation (DIM) for injection current of distributed feedback (DFB) laser or long-wavelength vertical cavity surface-emitting laser (LW-VCSEL). Hereinafter abbreviated as DIM-DFB or DIM-VCSEL, correspondingly.
- External intensity modulation (EIM) using electro-absorption modulator (EAM) or Mach-Zehnder modulator (MZM). Hereinafter abbreviated as EIM-EAM or EIM-MZM, correspondingly.

It should be noted that the key shortcomings of a DFB laser as compared to a LW-VCSEL are higher power consumption and substantially narrower band of

modulation [27]. On the contrary, the main preferences in terms of a signal transferring over an optical fiber consist in a smaller linewidth and a parasitic frequency modulation (chirp), which should lead to a significant extension in the permissible length of the FFL in the case of transmitting QAM signals. The quality is analyzed in terms of error vector magnitude (EVM) limit provided that the bottom of EVM value determined by the European Telecommunications Standard Institute (ETSI) corresponds to 8% for 64-QAM [28]. In all cases, the same 64-position QAM signal at the RF carrier in LR or HR (see **Figure 1**) will propagate over FFL.

We used the well-known commercial software VPIphotonics Design Suite™ as a tool for all computer simulation. Two key distortion sources are taken into account during the simulation procedure: a chirp of the lasers and modulators and a chromatic dispersion of the fiber. **Table 2** lists the common reference data for the FFL under study. In addition, **Tables 3** and **4** list the reference data for direct and external intensity modulation, correspondingly.

### 3.2 Proposed models and setups for simulation experiments

#### 3.2.1 Direct intensity modulation

**Figure 9** demonstrates VPIphotonics Design Suite’s direct intensity-modulated FFL model and setup that contain the library models of DFB laser or LW-VCSEL, standard single-mode optical fiber (SMOF), and pin photodiode followed by the RF amplifier model. Their relevant parameters are in **Tables 2** and **3**. Besides, the setup includes the library model of DC source to control the DC bias current of a laser.

Parameter		Value
Length of pseudorandom bit sequence		$2^{15}-1$
Bit rate		2.5 Gbit/s
RF carrier frequency		1.8–10, 15, 40 GHz
Input RF power		–10 to –20 dBm
Type of RF modulation		64-QAM
Optical carrier		C-band (1552.52 nm)
Optical modulation		Intensity
PIN photodiode	Responsivity	0.9 A/W
	Dark current	100 nA
	3 dB bandwidth	50 GHz
	Optical input power	<3 mW
Post-amplifier	Gain	30 dB
	Noise spectral density	$20 \times 10^{-12}$ A/Hz <sup>1/2</sup>
Optical fiber	Type	SMF-28e+
	Length	Up to 70 km
	Attenuation	0.2 dB/km
	Dispersion	$17e^{-6}$ s/m <sup>2</sup>
	Dispersion slope	80 s/m <sup>3</sup>

**Table 2.**  
Common reference data for the FFL under study.

Parameter	DFB		LW-VCSEL	
	Value	Reference	Value	Reference
Operating current	60 mA	—	9 mA	—
Linewidth	300 kHz	[29]	4.5 MHz	[27]
Relative intensity noise	−150 dB/Hz	—	−160	[27]
Threshold current	8 mA	[29]	2.5 mA	[27]
Slope efficiency	0.15 W/A	—	0.23 W/A	[27]
Linewidth enhancement factor ( $\alpha$ )	4.6	[30]	7.0	[31]
Adiabatic chirp factor ( $k$ )	3.2 GHz/mW	[30]	10 GHz/mW (at 1 GHz)	[31]

**Table 3.**  
*Reference data for direct intensity modulation.*

Parameter	EAM		MZM	
	Value	Reference	Value	Reference
Operating voltage	−0.5 V	—	−5.7 V	—
Extinction ratio	14 dB	[32]	25 dB	[33]
Slope efficiency	0.14 W/V	—	—	—
Linewidth enhancement factor ( $\alpha$ )	1.0	[34]	0 (X-cut)	[35]
Adiabatic chirp factor	0	[34]	—	—

**Table 4.**  
*Reference data for external intensity modulation.*

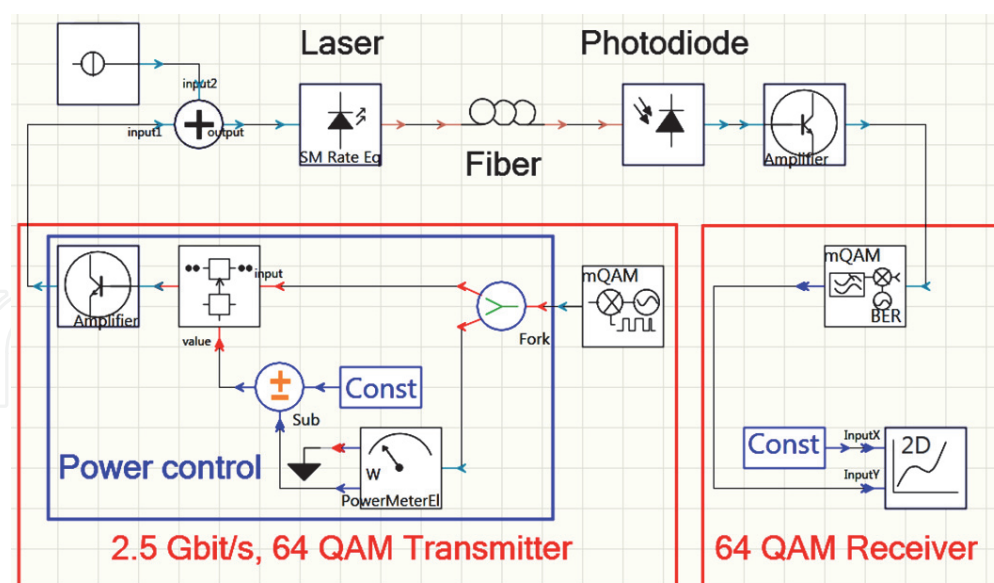


**Figure 9.** VPIphotonics design suite’s setup for a FFL with direct intensity modulation of QAM signals.

Finally, two instrumental library models are in the figure. The first one represents 2.5 Gbit/s, 64-QAM RF transmitter containing library model of QAM generator and output unit for power control. This module generates an electrical M-QAM signal up-converted at a desired frequency of the RF carrier. In addition, the second one represents electrical 64-QAM receiver. The module detects RF signal, decodes QAM signal, and evaluates the EVM of the QAM signal that has been transmitted. For

two-dimensional graphical representation of the data from the QAM receiver output, the model of numerical 2D analyzer is exploited.

3.2.2 External intensity modulation

**Figure 10** demonstrates VPIphotonics Design Suite’s external intensity-modulated FFL model and setup that contain the library models of EAM or MZM optically injected by C-band DFB laser. Their relevant parameters are in **Table 4**. Everything else in the figure coincides with the layout of **Figure 9**. Note that in the layout of **Figure 10**, the same DFB laser model as for direct intensity modulation is used, and its parameters are the same as in **Table 3** except the linewidth enhancement factor and the adiabatic chirp factor that are equal to zero.

3.3 Simulation results

**Figure 11** depicts the examples of simulating EVM vs. fiber length characteristics for all devices under study when transmitting QAM-modulated 1.8-GHz RF carrier. The figure also illustrates constellation diagrams at EVM = 2% for all devices and at EVM = 5.7% for EIM-EAM. As it follows, MZM-based external modulation has the best values of EVM. Somewhat worse EVM characteristics are obtained by modulation using EIM-EAM and DIM-DFB, and the largest values of EVM are provided by the direct modulation using LW-VCSEL, which coincides with the known data [30, 36].

Studying the optical transmission of QAM signals at higher frequencies of the RF carrier using the FFL models of **Figures 9** and **10**, we found an interesting effect that was observed only in the case of direct modulation using a LW-VCSEL (**Figure 12**). This effect consists in decreasing the steepness of the distance characteristic of EVM with increasing RF carrier frequency, while the similar characteristics for the other devices under study remained the same as in **Figure 11**. The most probable reason for this atypical behavior is explained by the inverse frequency dependence of the magnitude and phase of the adiabatic chirp factor for LW-VCSEL [31].

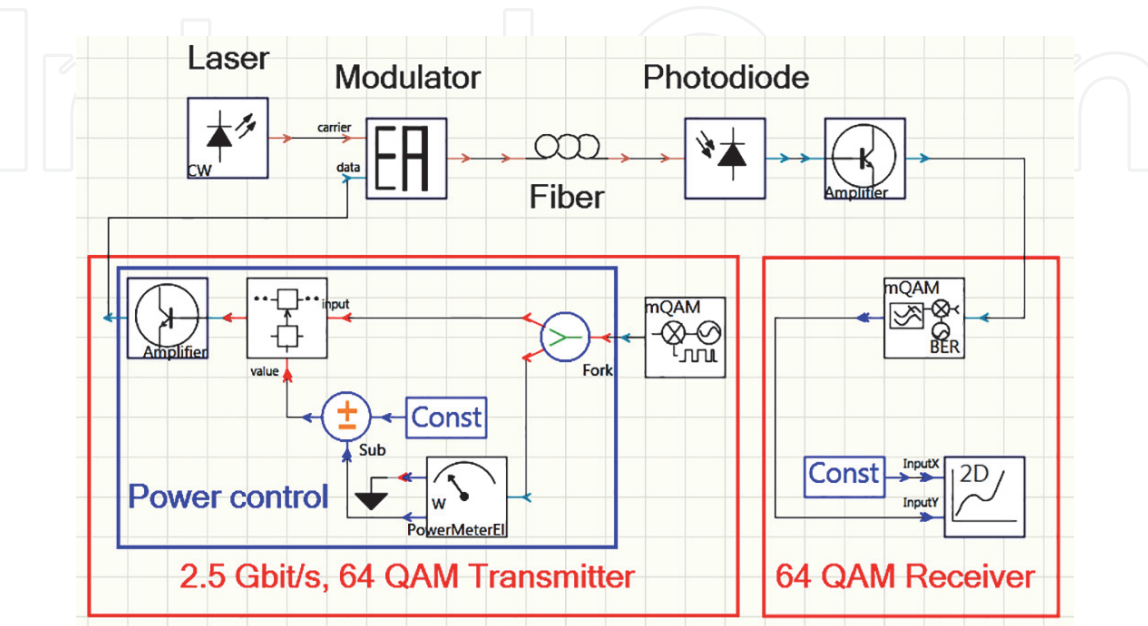


**Figure 10.**  
VPIphotonics design suite’s setup for a FFL with external intensity modulation of QAM signals.



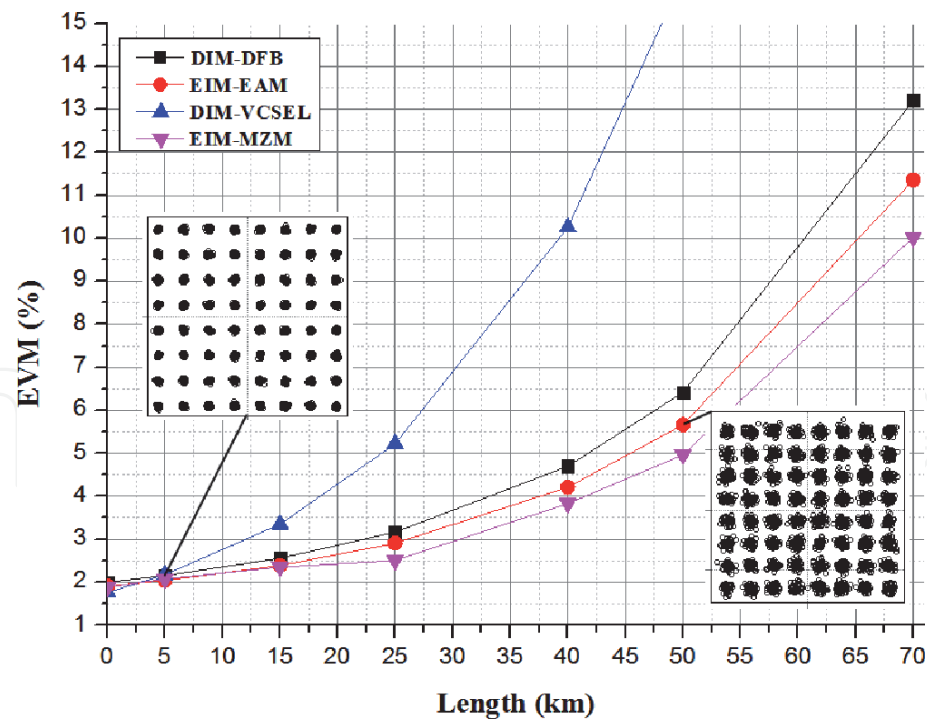


Figure 11. Examples of simulating EVM vs. fiber length characteristics.

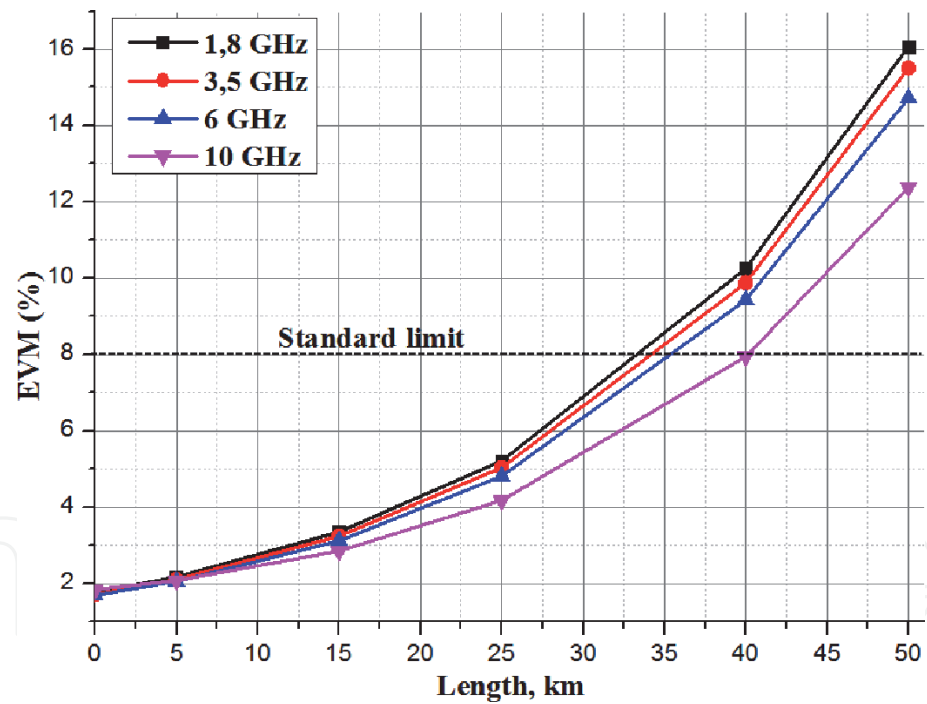


Figure 12. DIM-VCSEL’s EVM vs. fiber length characteristics at the various frequencies of RF carrier.

Some outcomes can be derived from the above analysis of the FFL under investigation:

- The allowable distance, when the standard EVM value during transmission of 64-QAM signal does not exceed 8% [28], is up to 62 km for an EIM-MZM, up to 58 km for an EIM-EAM, up to 55 km for a DIM-DFB, and up to 33 km for a DIM-VCSEL for the RF carrier of 1.8 GHz.
- At higher RF carrier frequencies up to 10 GHz, an atypical effect was detected for the direct modulation using a LW-VCSEL, which consists in a drop in the

slope of the EVM values with frequency increasing that is most likely explained by the presence of inverse frequency dependence of the adiabatic chirp factor’s magnitude and phase.

Leveraging the study, below the results of the simulation experiment by the same computer tool imitating transmission of quadrature amplitude-modulated RF signals of 40 GHz (HR of **Figure 1**) or 15 GHz (IF band) through a FFL-connected CS and RS are discussed. Because the direct modulation bandwidth of modern laser sources does not exceed 10–15 GHz, this experiment is performed only for a circuit with external modulation using three types of EOMs: double-sideband MZM (DSB MZM), carrier-suppressed single-sideband MZM (CS-SSB MZM), and EAM. **Table 5** lists the reference data for the modulators under test.

The remaining data correspond to **Table 2** except for the number of modulation positions (16-QAM instead of 64-QAM) and data rates (1.25 Gbit/s instead of 2.5 Gbit/s), which are selected from the point of view of practical work in the MMW band. The VPIphotonics Design Suite’s setup of the simulation experiment corresponds to **Figure 10**. **Figures 13, 14, and 15** depict examples of simulating EVM vs. fiber length characteristics for the modulator under test during optical

Parameter	DSB MZM	CS-SSB MZM	EAM
Optical insertion loss	4 dB	6 dB	3 dB
Optical extinction ratio	20 dB	20 dB	14 dB
Slope efficiency	—	—	0.14 W/V
RF $\pi$ -bias voltage	5.5 V	7.5 V	—
Electro-optical bandwidth	40 GHz	40 GHz	40 GHz
Linewidth enhancement factor ( $\alpha$ )	0 (X-cut)	0 (X-cut)	1.0

**Table 5.**  
Reference data for the modulators under test.

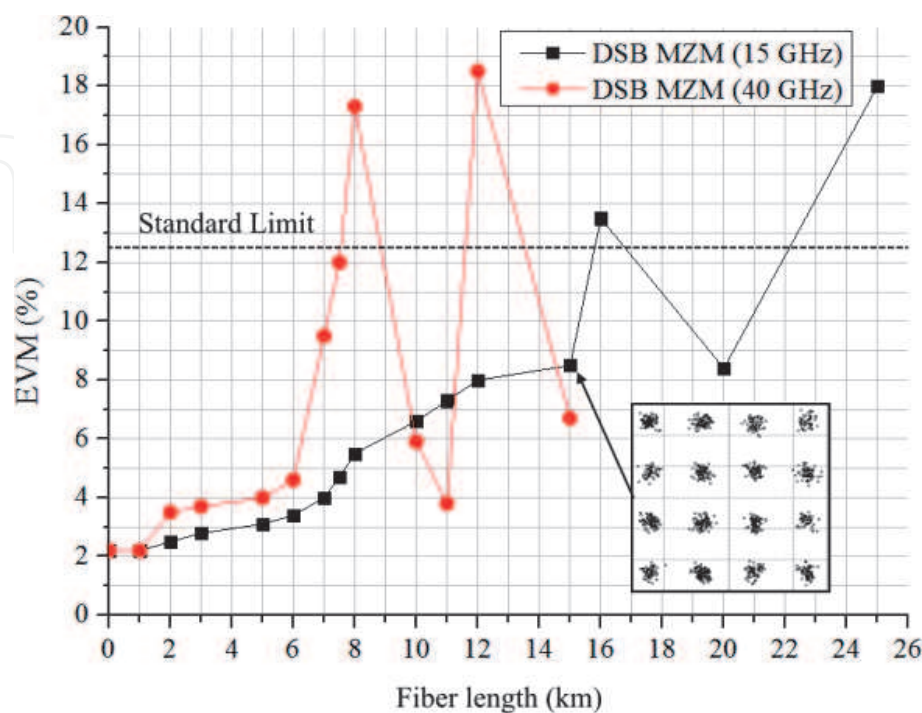


**Figure 13.**  
Example of simulating EVM vs. fiber length characteristic for a FFL with DSB MZM under test.

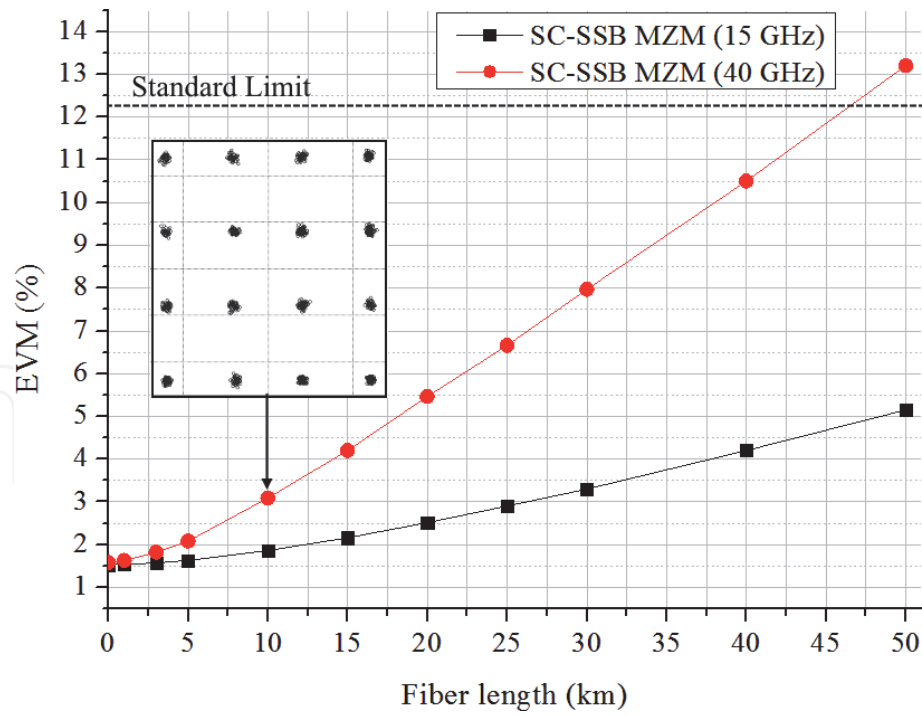


**Figure 14.**  
Example of simulating EVM vs. fiber length characteristic for a FFL with CS-SSB MZM under test.

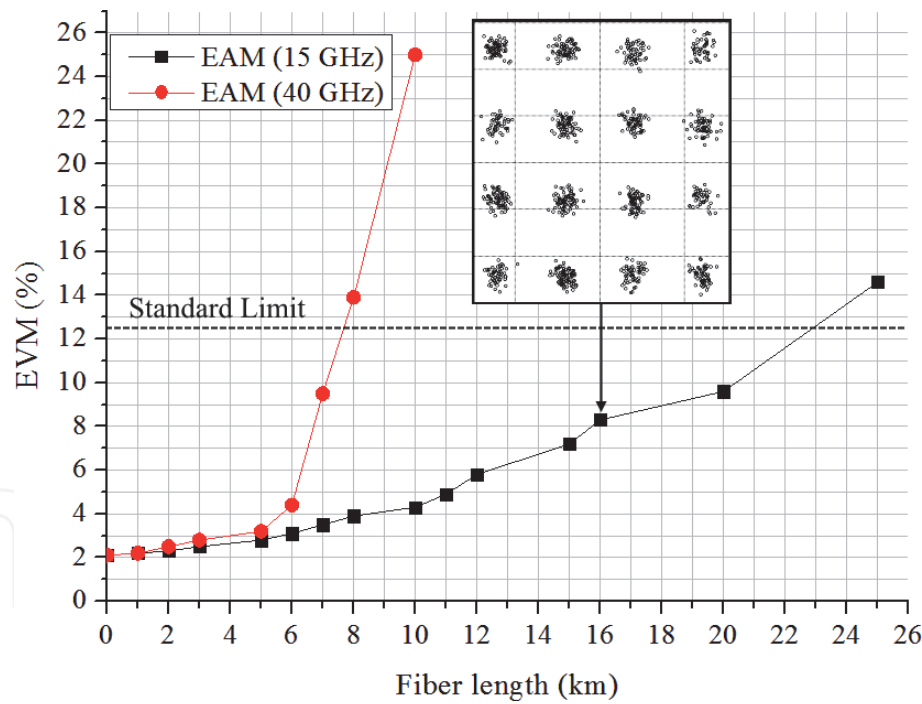


**Figure 15.**  
Example of simulating EVM vs. fiber length characteristic for a FFL with EAM under test.

modulation by 1.25 Gbit/s, 16-QAM, 15-GHz (transmission in IF band), or 40-GHz (transmission in MMW-band) RF signal, correspondingly. For the best vision, there are some insets in the figures showing constellation diagrams in specific points. In addition, in the figures, the dotted lines indicate the standard limit of the EVM during transmission of the 16-QAM signal, which is 12.5% [28].

The results of the simulation for the fiber-wireless fronthaul link of 5G NR system under study are summarized in **Table 6**.

The following outputs can be derived from our study:

- The minimum values of EVM were obtained for external modulation using CS-SSB MZM, which, nevertheless, requires the most complex control schematic, accordingly, and has the greatest value.
- The slope of the EVM characteristic increases with distance from SC-SSB MZM to DSB MZM through EAM, which corresponds to the known data [30, 34].
- The significant fluctuations in the values of the EVM at the 40-GHz RF carrier (see **Figure 13**) are characterized by the effect of dispersion in an extended optical fiber. To eliminate it in order to increase the length of the FFL, it is required to introduce at its end a dispersion corrector, which is a standard element in a fiber-optic communication system.

### 3.4 Design of fiber-to-MMW-band wireless interface

An important element of a RoF-based mobile communication network (see **Figure 3**) is a remote station, through which an interactive fiber-wireless interface is implemented. Recently, we have proposed and previously investigated advanced design concept of cost- and power-efficient base station for emerging FiWi networks, in which for a multifrequency conversion of a RF carrier, a MWP-assisted optical frequency comb generator (OFCG) based on an optical recirculation loop (ORL) technique using two SC-SSB optical modulators was developed [19]. Leveraging the application of this OFCG for a realistic case, the simulation results by the same computer tool imitating multiwavelength optical frequency comb generation and transmission of quadrature amplitude-modulated RF signals through OFCG-based FWI of a FiWi-architected RS are discussed.

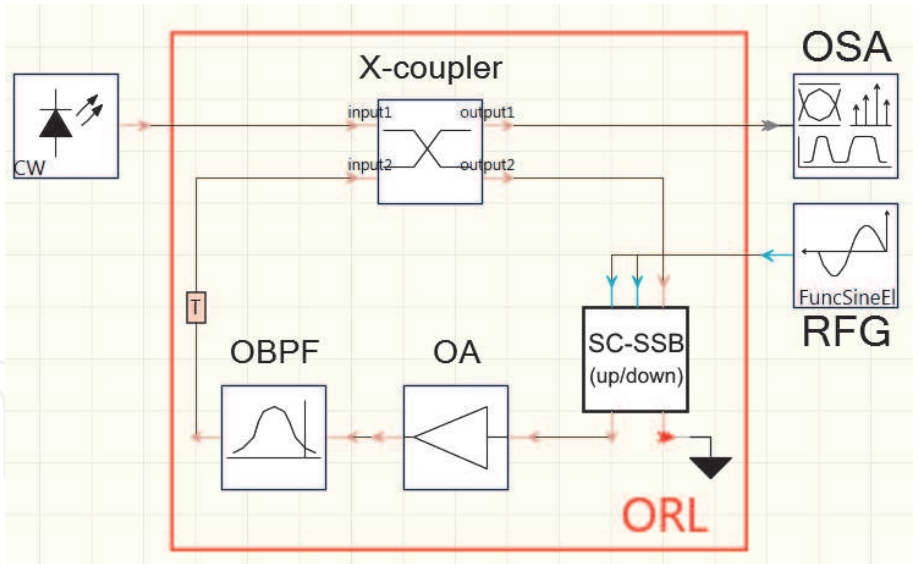
**Figure 16** shows the VPI model and setup for simulation of the OFCG scheme under study. There are four units depicted in the figure: the composed model of ORL includes library models of optical X-coupler, SC-SSB modulator, optical amplifier (OA), and optical band-pass filter (OBPF), library models of continuous-wave semiconductor laser (CW-SL) emitting at the frequency  $\nu_0$  as an optical source, RF generator (RFG) as a RF signal source, and library instrumental model of optical spectrum analyzer (OSA). In order to close the ORL, the output of OBPF through the service unit T and input of SC-SSB are connected to X-coupler's port "input2" and port "output2," correspondingly. During the simulation, RFG acts as a source of the reference RF signal ( $f_{\text{ref}}$ ), while using the OSA, the output optical spectrum is recorded.

**Figure 17** shows the VPI model and setup for simulation of OFCG-based fiber-to-MMW-band wireless interface, while transmission of QAM-modulated RF signals is supported. The scheme represents the downlink channel of FiWi-architected

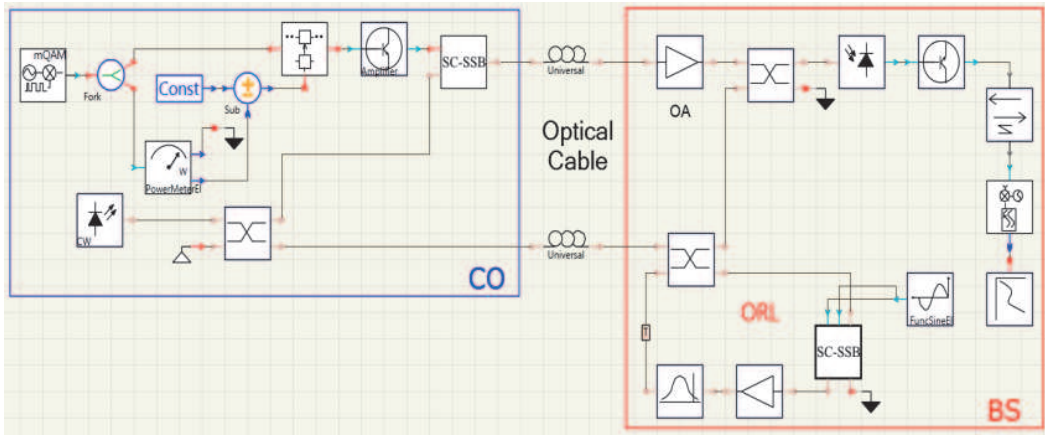
Device under test	RF carrier (GHz)	Allowable distance of FFL (km)
DSB MZM	15	16
	40	7.3
SC-SSB MZM	15	Much more than 50
	40	47
EAM	15	23
	40	8

Table 6.  
The results of the simulation.





**Figure 16.**  
VPI model and setup for simulation of the OFCG.



**Figure 17.**  
VPI model and setup for simulation of OFCG-based fiber-to-MMW-band wireless interface.

RoF system and consists of three units imitating the operation of CS, RS, and two-fiber optical cable between them. The CS includes the same laser model, the radiation of which is divided into two branches using a Y-coupler, library model of SC-SSB modulator with suppressing lower sideband and library instrumental model of QAM RF transmitter. The latter contains library models of QAM generator and output unit for power control followed by electrical amplifier. This module generates an electrical M-QAM signal up-converted at a given RF carrier frequency. The optical cable includes two equivalent library models of single-mode optical fiber. Such a remote optical feed reduces the cost of the RS. Besides the OFCG model (see **Figure 16**), the RS includes library models of optical amplifier, X-coupler, photodiode, and electrical post-amplifier outputted to the model of QAM RF receiver (see Section 3.1).

In the course of the research, first of all, the possibility of creating a multifrequency OFCG with the closest arrangement of the teeth is checked. Then, the transmission quality of a digital RF signal with multi-position QAM through the downlink channel of the RS using fiber-to-MMW-band wireless interface is analyzed. **Table 7** lists the common reference data for the OFCG under study. The reference data for the fiber-to-MMW-band wireless interface under study correspond to **Table 2**, with the exception of the frequency of RF carrier (37–43.5 GHz instead of 1.8–40 GHz) and data rates (1.25 Gbit/s instead of 2.5 Gbit/s).

**Figure 18** demonstrates an OSA’s spectrum of multiwavelength optical frequency comb output following the setup of **Figure 16**. As one can see from the figure, the OFCG under study includes 21 optical carriers with the spacing of 0.3 GHz and a level nonuniformity of less than 5 dB.

The results of the simulations are presented in **Figure 19**. For a clear view, there are some insets in **Figure 19** showing constellation diagrams in specific points. In particular, as one can see from the figure, due to dispersion in the optical cable, the EVM values increase with a slope of near 0.17%/km reaching a standard limit for 64-QAM of 8% [28] at a distance of 40 km.

The following output can be derived from our study. When transmitting digital radio signals with 64-QAM on millimeter-wave RF carriers (37–43.5 GHz), even when using SC-SSB MZM and high coherent laser, the dispersion in an optical cable has a significant impact on the quality of the received signal. However, the error is within the standard limit up to a distance of 40 km.

3.5 Studying an optimal signal transmitting RoF-based fiber-to-MMW-band wireless interface

Finally, we consider and discuss the optimal design principle of an interactive fiber-wireless fronthaul network when distributing digital radio signals over fiber-optic link. The feasible variants are compared in **Table 8**. For the possibility of quantitative analysis, we take the widely used bitrate for the modern networks of 1 Gbit/s (e.g., the standard Gigabit Ethernet).

Parameter	Value
Laser source frequency ( $\nu_0$ )	193.3 THz
Laser linewidth	10 kHz
Reference RF frequency ( $f_{\text{ref}}$ )	0.3 GHz
Type of modulator inside optical recirculating loop	SC-SSB (up/down)
Gain of recirculating loop (g)	$0.8 < g < 1$
Number of up or down round trips	Not less than 10
Level nonuniformity of output comb teeth	Not more than 5 dB

**Table 7.**  
Reference data for the OFCG under study.

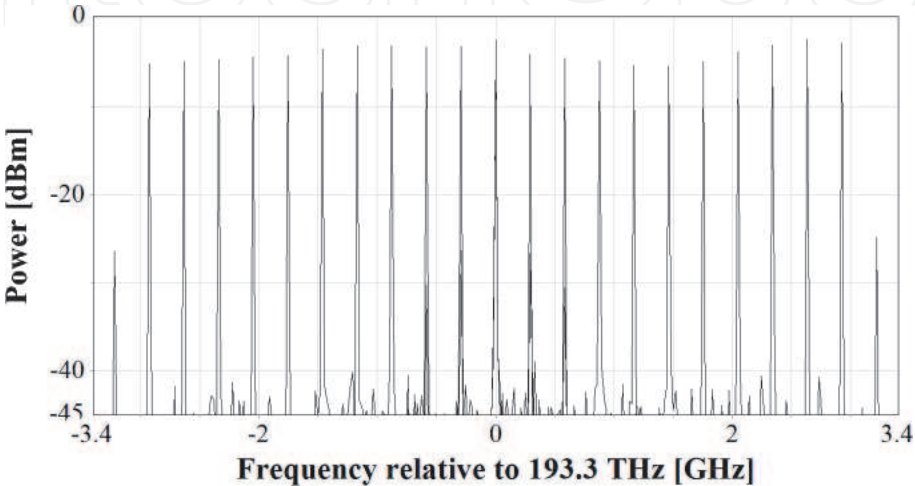


**Figure 18.**  
A spectrum of multiwavelength optical frequency comb output.

Based on the general comparison, below the results of our recent investigations to design optimally a fiber-wireless fronthaul including a central station, MMW wireless interface, and pico-cell remote station are presented.

In particular, we compare the three options of distributing signals through fifth-generation fronthaul communication network of fiber-wireless architecture with a wireless section operating in MMW band: in baseband, in intermediate frequency band, and directly in RF band on the same MMW frequencies. **Figure 20** demonstrates three possible options including interactive transmission in the baseband (a), in the IF band (b), and in the RF (MMW) band (c). The following abbreviations are used in the figure: TSL, tunable semiconductor laser; EOM, electro-optic modulator; PD, photodetector; RFM, RF modulator; RFDM, RF demodulator; MIMO, multiple input/multiple output; IFM, IF modulator; RFC, RF converter.

To verify the optimal layout, a transmission quality simulation of a 64-QAM, 2.5 Gbit/s digital signal transmitted at a frequency in the IF band (15 GHz) or in the

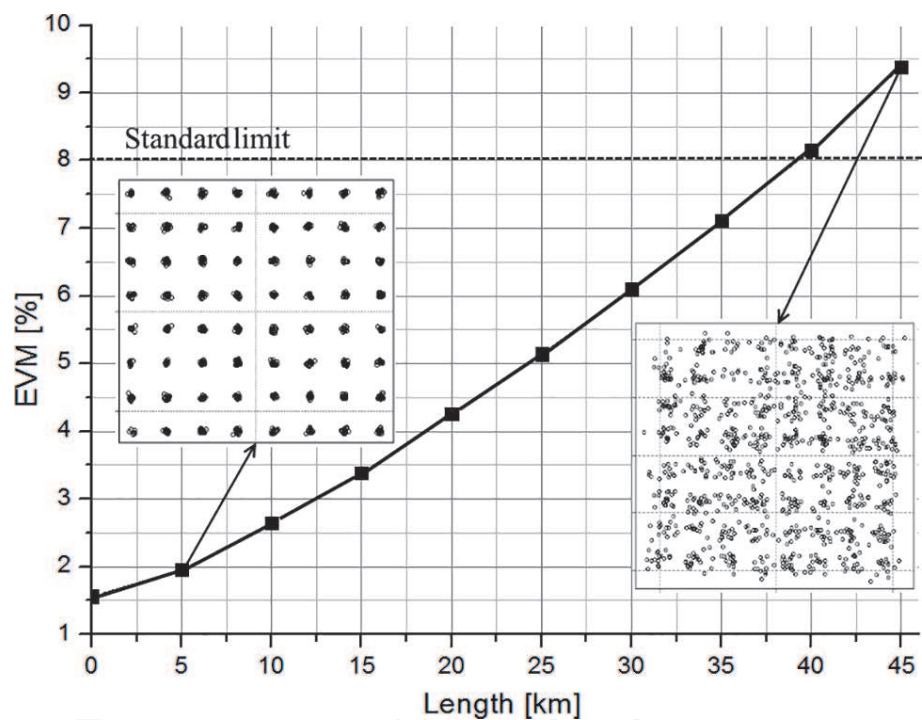


**Figure 19.**  
*EVM vs. optical cable length.*

Transmission range	Option 1. In baseband	Option 2. In the band of intermediate RF signals	Option 3. In the band of RF carriers
Type of FOCS	Digital	Analog	Analog
Upper modulation frequency (GHz)	1	10–15	40–80
Relative bandwidth (%)	100	40	30
Demands to signal-to-noise ratio	Low	High	High
Demands to the equipment linearity	Low	High	Middle
Complexity of CO layout (cost)	Low	Middle	High
Complexity of BS layout (cost)	High	Middle	Low

**Table 8.**  
*Comparison of the feasible options for transporting signals over FWI.*

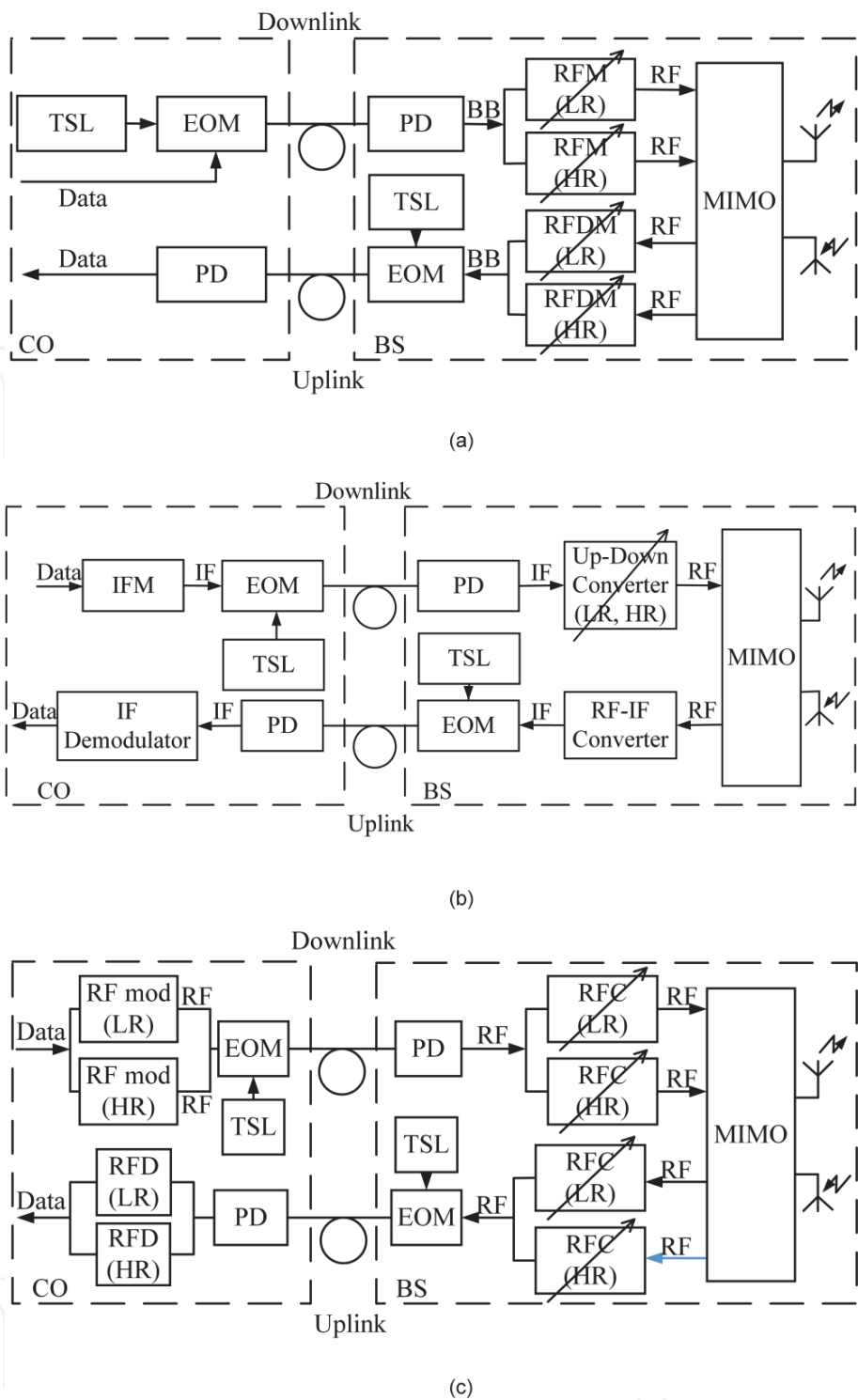


**Figure 20.**  
The possible options of transmitting signals through FiWi fronthaul. (a) Baseband-over-Fiber transmission, (b) IF-over-Fiber transmission, and (c) RF-over-Fiber transmission.

MMW band (40 GHz) through FFL using CS-SSB MZM, was performed by the same off-the-shelf computer tool of VPIphotonics Design Suite. The reference data used in the calculations are taken from **Table 5** for the modulator and from **Table 2** for the entire FWFN. The result, which is a dependence of the EVM vs. the fiber length, is shown in **Figure 21**.

As follows from the figure, the transmission at 40 GHz is carried out at a much worse quality than at 15 GHz. In particular, the standard for 64-QAM limit of 8% [28] is achieved in the first case with a fiber link length of 23 km and as much as 60 km in the second case.



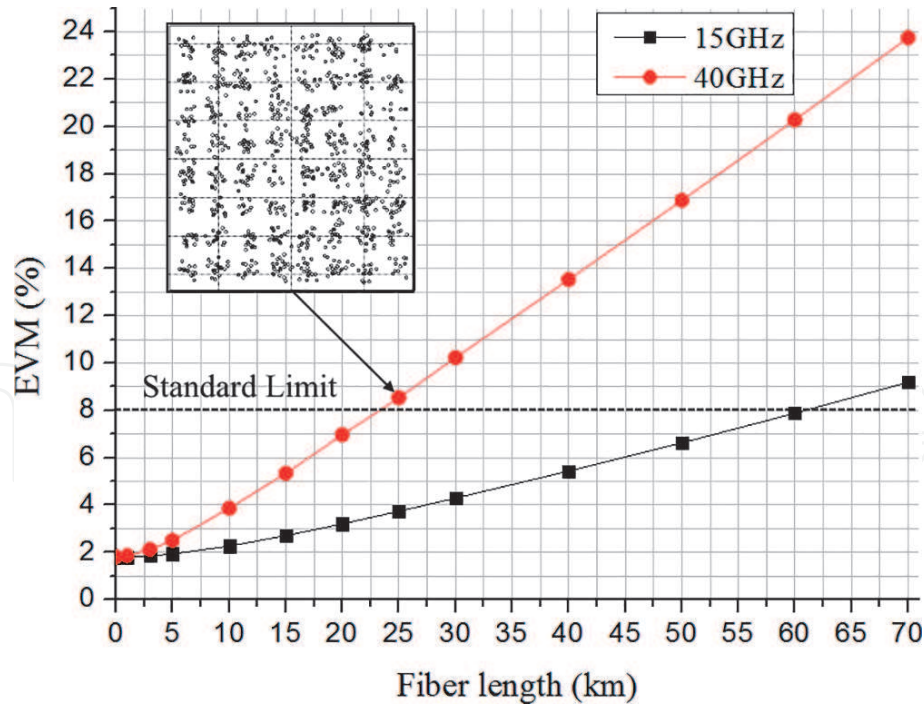


**Figure 21.**  
*EVM vs. fiber length characteristic.*

The following outcomes can be drawn:

- To realize Option 1, it is necessary to use digital fiber-optic communication system, whereas for the second and third options, analog system is required with its inherent higher requirements for the signal-to-noise ratio and the linearity of the equipment.
- The value of the upper modulation frequency in the second and, especially, in the third options is significantly higher in comparison with the first one, which tightens the requirements for the electronic and optoelectronic components of the CS equipment and, as a result, its cost.
- The relative bandwidth of the transmission channel for the second and third options is substantially lower than in the first one, which simplifies the circuitry of the CS and RS equipment's amplifying and converting units and, as a result, improves their cost characteristics.
- The option with transmission in the RF carrier band is realized with the least number of transformations on the RS, which minimizes its cost and, consequently, the cost of the entire user access network. However, the fiber-optic transmission of the MMW-band signals has a serious limitation due to the dispersion effect of standard optical fiber.

We believe that the optimal approach would be IF-over-fiber transmission in spite of this option requiring an interface at the RS that has to perform RF up- or down-conversion. Nevertheless, transmission in IF band (see **Figure 20(b)**) provides versatility, as there is a simple possibility of RF conversion at a RS, both in the LR and in the HR (see **Figure 1**). For the effective implementation of it, we have proposed and described two RS schemes [14, 19] capable of frequency converting both LR and HR.

## 4. Conclusion

In the chapter, we proposed and highlighted in detail the specific for incoming fifth-generation mobile communication system principles to optimally design an access network using small cell scenario, radio-over-fiber concept, and microwave-photonic-based approach. In the generally accepted interpretation, the small cell scenario means a consistent network partitioning into micro- and pico-cells with a service area diameter of not more than 200 m. Radio-over-fiber concept is to design pico-cell network based on fiber-wireless architecture. Using microwave-photonic-based approach means the formation and processing of transmitted radio signals in the optical range, which leads to a significant improvement of the bandwidth features at lower size, weight, and power as compared with traditional characteristics of network equipment. The main idea behind the proposed principle to design pico-cell fiber-wireless fronthaul network is to split it into two sub-systems that consist of optical distribution network including central station hardware and fiber-optic link and fiber-wireless interface including a remote station hardware and the same fiber-optic link. In order to verify efficiency of the proposed design principles, we performed modeling in a well-known computer-aided design environment VPIphotonics Design Suite. The goal of the study was to examine and select optimal modulating scheme and transmitter parameters to propagate higher-order quadrature amplitude modulation signals at radio-frequency carriers of millimeter-wave band over radio-over-fiber-based fiber-wireless Fronthaul network using advanced commercial optoelectronic devices and standard single-mode optical fiber. In the result of simulation experiments, optimal design principles of optical distribution network, fiber-wireless interface, and fiber-wireless fronthaul network as a whole have been proposed, described, and validated. Particularly, the study of the optimal method and device for transmitting multi-positional QAM signals at RF carriers showed that in the so-called low range (see **Figure 1**), the maximum allowable distance of a fiber-optic link is provided up to 33 km for a LW-VCSEL and up to 55 km for a DFB laser in the case of direct modulation, as well as up to 58 km for an EAM and up to 62 km for a SC-SSB MZM in the case of external modulation. In addition, in the so-called high range (see **Figure 1**), the maximum allowable distance of a fiber-optic link is significantly reduced, reaching at best not more than 23 km even when using a SC-SSB MZM, which, nevertheless, requires the most complex control schematic, accordingly, and has the greatest value.

## Acknowledgements

This work was supported by the Russian Foundation for Basic Research, Grant No. 18-29-20083.

## Conflict of interest

The authors declare the lack of the “conflict of interest.”

IntechOpen

IntechOpen

### **Author details**

Mikhail E. Belkin\*, Tatiana N. Bakhvalova and Alexander S. Sigov  
Scientific and Technological Center “Integrated Microwave Photonics”,  
MIREA-Russian Technological University, Moscow, Russian Federation

\*Address all correspondence to: [belkin@mirea.ru](mailto:belkin@mirea.ru)

### **IntechOpen**

---

© 2019 The Author(s). Licensee IntechOpen. This chapter is distributed under the terms of the Creative Commons Attribution License (<http://creativecommons.org/licenses/by/3.0>), which permits unrestricted use, distribution, and reproduction in any medium, provided the original work is properly cited. 

## References

- [1] Andrews JG, Buzzi S, Choi W, Hanly SV, Lozano A, Soong ACK, et al. What will 5G Be? *IEEE Journal on Selected Areas in Communications*. 2014;**32**(6):1065-1082
- [2] Chen S, Zhao J. The requirements, challenges and technologies for 5G of terrestrial mobile telecommunication. *IEEE Communications Magazine*. 2014;**52**(5):36-43
- [3] Munn J. Our 5G future: In the fast lane with numerical simulation. *Microwaves & RF*. 2016;**16**:48-50
- [4] Frenzel L. Making 5G happen. *Microwaves & RF*. 2017:1-5
- [5] Browne J. What role will millimeter waves play in 5G wireless systems? *Microwaves & RF*. 2018;**10**:38-42
- [6] Waterhouse R, Novak D. Realizing 5G. *IEEE Microwave Magazine*. 2015;**16**(8):84-92
- [7] Boccardi F, Heath RW, Lozano A, Marzetta TL, Popovski P. Five disruptive technology directions for 5G. *IEEE Communications Magazine*. 2014;**52**:74-80
- [8] Novak D, Waterhouse R. Emerging disruptive wireless technologies—Prospects and challenges for integration with optical networks. In: *IEEE: 2013 Optical Communication Conference and Exposition and the National Fiber Optic Engineers Conference (OFC/NFOEC)*. Anaheim, CA, USA. 17–21 March. 2013. pp. 1-3. DOI: 10.1364/OFC.2013.OTu3E.2
- [9] World Radiocommunication Conference 2019 (WRC-19). Available at: <https://www.itu.int/net/events/eventdetails.asp?eventid=14719> [Accessed: 23 September 2019]
- [10] ITU. Final acts of WRC-2015 World Radiocommunication Conference. Resolution 238, Geneva 2016. pp. 296-298
- [11] Novak D et al. Radio-over-fiber technologies for emerging wireless systems. *IEEE Journal of Quantum Electronics*. 2016;**52**(1):1-11
- [12] Al-Raweshidy H, Komaki S, editors. *Radio over Fiber Technologies for Mobile Communications Networks*. Norwood: Artech House; 2002. 436 pp
- [13] Sauer M, Kobayakov A, George J. Radio over fiber for picocellular network architectures. *IEEE Journal of Lightwave Technology*. 2007;**25**(11): 3301-3320
- [14] Belkin ME. The building principles of a cost- and power-efficient base station for emerging fiber-wireless networks. In: *International Conference on Microwaves, Communications, Antennas and Electronic Systems, COMCAS 2017*; 13–15 Nov. 2017; Tel Aviv, Israel. pp. 1-4
- [15] Belkin ME, Golovin V, Tyschuk Y, Sigov AS. Studying an optimal approach to design combined fiber-wireless telecom systems. In: *41st International Conference on Telecommunications and Signal Processing, TSP 2018, Athens, July 4–6. 2018*. pp. 43-46
- [16] Belkin ME, Fofanov D, Golovin V, Tyschuk Y, Sigov AS. Design and optimization of photonics-based beamforming networks for ultra-wide mmWave-band antenna arrays. In: *Array Pattern Optimization*. United Kingdom, London: IntechOpen; 2018. pp. 47-67 Available from: <https://www.intechopen.com/online-first/design-and-optimization-of-photonics-based-beamforming-networks-for-ultra-wide-mmwave-band-antenna-a>
- [17] Fofanov DA, Bakhvalova TN, Alyoshin AV, Belkin ME, Sigov AS.



Studying microwave-photonics frequency up-conversion for telecom and measurement equipment. In: IEEE Radio and Antenna Days of the Indian Ocean (RADIO2018), Mauritius. 2 pp.

[18] Bakhvalova T, Belkin M, Fofanov D. Advances in fiber-wireless network architecture approach to the next-generation communication systems. In: Proceedings of the Seventh International Conference on Advances in Computing, Communication and Information Technology—CCIT; 27–28 October 2018. Rome, Italy. 2018. pp. 62-67

[19] Belkin ME, Bakhvalova T, Turitsyn S, Sigov A. The design principles of reconfigurable versatile base station for upcoming communication networks. In: 26th Telecommunications Forum (TELFOR2018), Belgrade, Serbia. Nov. 2018. pp. 180-182

[20] Fofanov DA, Bakhvalova TN, Alyoshin AV, Belkin ME. Microwave-photonics frequency up-converter for telecom and measurement equipment. IOP Conf. Series: Materials Science and Engineering. 2019;524:-012006

[21] Belkin M, Bakhvalova T. Microwave photonics and fiber-wireless interface—A principal approaches to design millimeter-wave network equipment for the next-generation wireless communication systems. In: Proceedings of the eighth International Conference on Advances in Computing, Communication and Information Technology—CCIT, 23–24 April 2019, Birmingham, UK. pp. 27–31

[22] Bakhvalova TN, Fofanov DA, Alyoshin AV, Belkin ME. Fiber distribution networks with direct and external modulation by digital QAM-signals. In: Proceedings of the 42nd International Conference on Telecommunications and Signal Processing (TSP2019), 1–3 July 2019. Budapest, Hungary; 2019. pp. 241-244

[23] Belkin M, Bakhvalova T. Studying optical frequency comb-based fiber to millimeter-band wireless interface. In: The Fifteenth Advanced International Conference on Telecommunications (AICT-2019), 28–31 July 2019. Nice, France; 2019. pp. 94-98

[24] Belkin M, Bakhvalova T, Sigov A. Studying an optimal approach to distribute signals through fiber-wireless Fronthaul network. In: IEEE Conference on Microwaves, Communications, Antennas and Electronic Systems (COMCAS-2019), November 4-6, Tel Aviv, Israel. 2019. in press

[25] Dat PT, Kanno A, Kawanishi T. Radio-on-radio-over-fiber: Efficient fronthauling for small cells and moving cells. IEEE Wireless Communications. 2015;22:67-75

[26] Dat PT, Kanno A, Umezawa T, Yamamoto N, Kawanishi T. Millimeter-and terahertz-wave radio-over-fiber for 5G and beyond. IEEE Photonics Society Summer Topical Meeting. August 2017:21

[27] Belkin ME, Belkin L, Loparev A, Sigov AS, Iakovlev V. Long wavelength VCSELs and VCSEL-based processing of microwave signals. In: Pyshkin S, Ballato J, editors. Optoelectronics—Advanced Materials and Devices. Croatia: InTechOpen; 2015. pp. 231-250 Chapter 6

[28] ETSI. Minimum requirements for Error Vector Magnitude. In Technical Specification, LTE; Evolved Universal Terrestrial Radio Access (E-UTRA); User Equipment (UE) radio transmission and reception (3GPP TS 36.101 version 14.3.0 Release 14), ETSI, 2017-04, p. 215

[29] Laserscom LDI-1550-DFB-2.5G Data sheet. Available at: [www.laserscom.com](http://www.laserscom.com)

[30] Kim BG, Bae SH, Kim H, Chung YC. RoF-based mobile Fronthaul networks implemented by using DML and EML

for 5G wireless communication systems.  
IEEE Journal of Lightwave Technology.  
2018;**36**(14):2874-2881

[31] Halbritter H, Shau R, Riemenschneider F, Kogel B, Ortsiefer M, Roskopf J, et al. Chirp and linewidth enhancement factor of 1.55  $\mu\text{m}$  VCSEL with buried tunnel junction. Electronic Letters. 2004; **40**(20):1266-1268

[32] Optilab EML. OL5158M-LC Data sheet. Available at: [www.optilab.com](http://www.optilab.com)

[33] iXblue Photonics LiNbO<sub>3</sub> modulator MXER-LN-10. Available at: <https://photonics.ixblue.com/>

[34] Salvatore RA, Sahara RT, Bock MA, Libenzon I. Electroabsorption modulated laser for long transmission spans. IEEE Journal on Quantum Electronics. 2002;**38**(5):464-476

[35] Koyama F, Iga K. Frequency chirping in external modulators. IEEE Journal of Lightwave Technology. 1988; **6**(1):87-93

[36] Mikroulis S, Karabetsos S, Pikasis E, Nassiopoulou A. Performance evaluation of a radio over fiber (RoF) system subject to the transmitter's limitations for application in broadband networks. IEEE Transactions on Consumer Electronics. 2008;**54**(2):437-443